ELSEVIER

Journal of Molecular Catalysis A: Chemical 167 (2001) 157–163

JOURNAL OF MOLECULAR CATALYSIS A: CHEMICAL

www.elsevier.com/locate/molcata

A statistical model for flash thermal desorption of carbon dioxide from polycrystalline molybdenum

L.D. López-Carreño [a,1], A.J. Ramírez-Cuesta [b], L. Viscido [a], J.M. Heras [a,*]

[a] *Institute of Physical Chemistry (INIFTA), University of La Plata, CONICET, CICPBA, C.C.16 Sucursal 4 (1900), La Plata, Argentina*

[b] *Department of Chemistry, University of Reading, Whiteknights, P.O. Box 224, Reading RG6 6AD, UK*

Received 21 June 2000

Abstract

The interaction of CO_2 with a polycrystalline molybdenum-foil (Mo-foil) was previously studied at 77 K through mass-resolved flash thermal desorption spectroscopy (FTDS). From the results, a statistical model was developed with two kinds of sites (bridge and hollow type), CO_2 can adsorb on both but dissociates only on hollow ones. The proposed model reproduces the evolution of desorption peak areas as a function of CO_2 exposure without using any fitting parameter. Because of the sample polycrystallinity, all desorption peaks were fitted assuming a Gaussian distribution of desorption energies with a pre-exponential factor of 10^{13}. Values of ∼60.6, ∼126.9 and ∼158.7 kJ/mol were obtained for the desorption energies of CO_2 from α_1, β_1 and γ_1 states, respectively, while 73.1 and 110.6 kJ/mol correspond to the CO α_2 and β_2 desorption peaks.

Keywords: Modeling flash desorption; Carbon monoxide; Carbon dioxide; Molybdenum

1. Introduction

The study of CO_2 interaction with metal surfaces has awakened a great experimental [1–7] and theoretical [8] interest, mainly because of the possibility of its use as an inexpensive reactant in methanation reactions [9,10]. In contrast with CO [11], little work has been devoted to the adsorption of CO_2 on Mo [7]. In a previous paper [12] we reported on the interaction of CO_2 molecules with a thin polycrystalline molybdenum-foil (Mo-foil) at 77 and 130 K, studied through Auger electron spectroscopy (AES), mass resolved flash thermal desorption (FTD) and work function (WF).

The present paper deals with the statistical modeling of the FTD results, under the principal assumption of two types of adsorption sites: the bridge and the hollow ones. CO_2 can adsorb on both but it can decompose only on hollow sites. The model accounts not only for the relation between the intensity of the β_1 to the γ_1 CO_2 desorption peaks but also for the dependence of the CO peaks intensity on CO_2 exposure. A quantitative evaluation of the desorption peaks can be made if a continuous distribution of adsorption energies is proposed for each type of adsorption sites. This

* Corresponding author. Fax: +54-221-425-4246.
E-mail address: surfaces@inifta.unlp.edu.ar (J.M. Heras).
[1] Present address: Department of Physics, Universidad Nacional de Colombia, Santafé de Bogotá de Bogotá, Colombia.

1381-1169/01/$ – see front matter
PII: S1381-1169(00)00502-1

proposal, based on the broad peak widths, can be justified considering the Mo-foil polycrystallinity which implies different environments for the adsorption sites.

2. Experimental details

The experimental UHV system has been explained in detail elsewhere [12,13]. The sample, a polycrystalline Mo-foil (Goodfellow Metals 99.9% pure, 10 mm × 10 mm × 0.05 mm) was characterized by photoelectric absolute WF measurements and X-ray diffraction (XRD) procedures in a vertical goniometer device (XRD).

The photoelectric WF is a surface property suitable to follow not only contamination but also surface structure changes upon annealing [14]. The WF of the clean Mo surface was 4.61 eV in good agreement with published results for polycrystalline sheet surfaces [15], while that of the surface contaminated with C and O was 5.09 eV. The first value was used to check that the adsorption–desorption cleaning cycles caused no change in the surface structure. In separate experiments in which surface purity was controlled with Auger spectroscopy [12], it was stated that a WF value of 4.61 eV indicates an extremely clean surface.

XRD was used to control lattice parameters, texture effects and the average crystallite size. The lattice parameter a_0 obtained with the least squares method of Cohen was 314.71 pm, in good agreement with published results (a_0=314.72 pm, [16]). Fig. 1 shows in part (a) the experimental diffraction pattern of the Mo-foil and in part (b) the pattern of the standard random oriented powder [17]. Evidently, the second order reflection of the (1 0 0) planes (first order not appearing because of systematic absences in bbc-structures) is the leading peak, in contrast with the random oriented crystallites of the standard powder. This fact clearly indicates a preferential orientation of the crystallites in the Mo-foil, which undoubtedly can be ascribed to the rolling process. Actually, in bbc metals like Mo, the rolling direction is [1 1 0] causing the (1 0 0) planes to orientate parallel to the resulting sheet surface [18]. The (2 0 0) reflection was also used to determine D, the average crystallite diameter parallel to the foil surface, according to the Scherrer equation, and using a Mo(1 0 0) single crystal to determine the pure diffraction peak width. The value obtained was

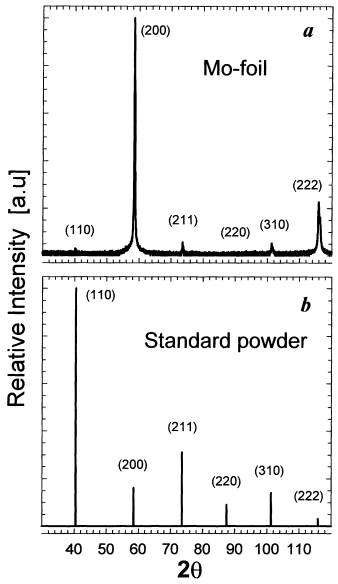

Fig. 1. XRD pattern of the Mo-foil sample compared to that of a standard random oriented powder. The leading (2 0 0) peak indicates a rolling texture.

$D = 60$ nm. Accordingly, the mean number of hollow sites per (1 0 0) oriented crystallite is $\sim 3 \times 10^4$, while for crystallite border sites it amounts $\sim 6 \times 10^2$. This last type of sites will show a higher coordination number than that offered by the Mo(1 0 0) hollow sites, possibly equal to or higher than the number of hollow sites provided by the Mo(1 1 1) planes, whose small contribution is represented in Fig. 1 by the second order peak (2 2 2). It is expected that they both will contribute to high temperature tails in the desorption spectra. From what has been said above, it follows that the ratio between the bridge:hollow:border type of sites offered by the polycrystalline Mo-foil used is approximately given by 100:50:1 (including a rough estimation of the contribution of the (1 1 1) planes).

FTD spectra were obtained at heating rates ∼100 K/s following adsorption of high purity CO_2 (4.5N, Messer-Griesheim, Germany) with the sample at 77 K. The exposures, between 2–20 L, were performed at a constant CO_2 pressure of 2×10^{-8} mbar. The evolution of the desorption peaks was monitored mass spectrometrically at the mass channels e/m = 16, 28, 32 and 44, data were automatically acquired at 10 kHz. Desorption of O_2 was not detected, even at ∼1100 K. The electron-impact dissociation of the

CO_2 molecules produced within the mass spectrometer was taken into account.

3. Results and discussion

3.1. Statistical model

We have stated previously [12] that above three Langmuir (L) exposure to CO_2, three CO_2 desorption peaks could be distinguished during FTD, $\alpha_1 \sim 210$, $\beta_1 \sim 500$ and $\gamma_1 \sim 700$ K, assigned to physisorbed, chemisorbed and rebuilt CO_2, respectively. Fig. 2 shows the experimental results at 5, 10, 15 and 20 L exposures. Note that only the γ_1-peak is fitted with a Gaussian with an exponential modified tail (as given by the commercial software). Possibly, this modification is required by the presence of a number of sites with high coordination number (crystallite border sites and (1 1 1) planes). We shall address this issue later. Additionally, as a result of CO_2 decomposition above ~200 K, two CO desorption peaks were detected: $\alpha_2 \sim 230$ K and $\beta_2 \sim 310$ K, assigned to two different types of adsorption sites, as Fig. 3 shows. This figure gathers the experimental CO desorption data after the Mo sample has been exposed to 2, 4, 5 and 15 L of CO_2. In both figures the thick continuous line represents the experimental data and the thin curves the deconvolution using the Marquard-Levenberg algorithm.

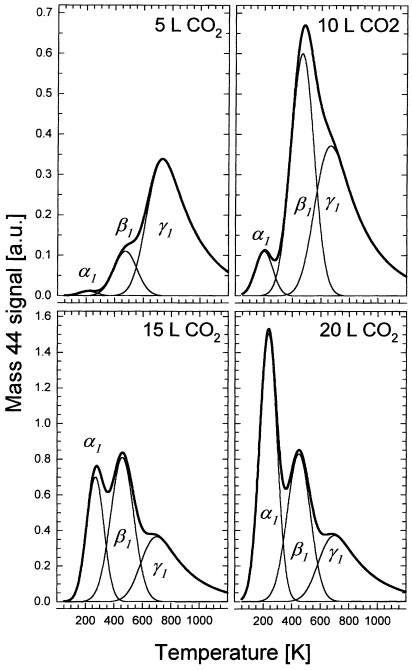

Fig. 2. Deconvolution of the CO_2 desorption spectra at the selected exposures indicated. The lower part of the figure has a wider ordinate scale.

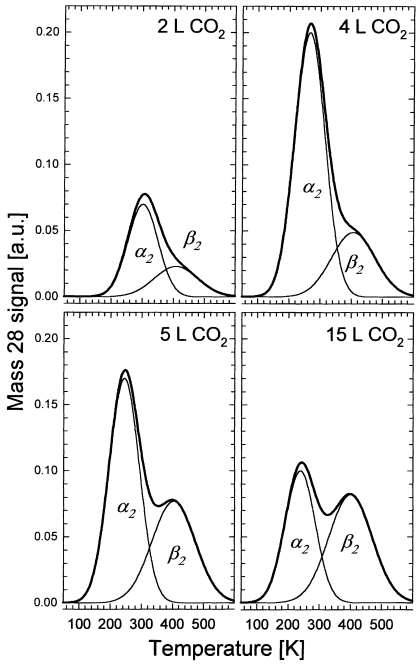

Fig. 3. Deconvolution of the CO desorption spectra after the Mo sample has been exposed to the indicated amount of CO_2 at 77 K.

From the FTD spectra, the evolution of the integrated intensity of each of the CO_2 and CO peaks (i.e. the area under each desorption peak) was calculated. This integrated intensity is proportional to the coverage θ and is shown in Fig. 4 as a function of the exposure to CO_2. In this figure the symbols represent the experimental data while the full lines indicate the predictions of the model to be developed later on. At exposures above 12 L the ratio between the integrated intensity of the CO_2 β_1 and γ_1 desorption peaks is 2:1. This fact suggests that the Mo surface offers principally two types of adsorption sites for the CO_2 molecule with a population of 2:1. Actually, the ratio of the bridge (*b*) to the hollow (*h*) sites of the Mo(1 0 0) plane satisfies this requirement. Remarkably, as explained above, XRD spectra of the

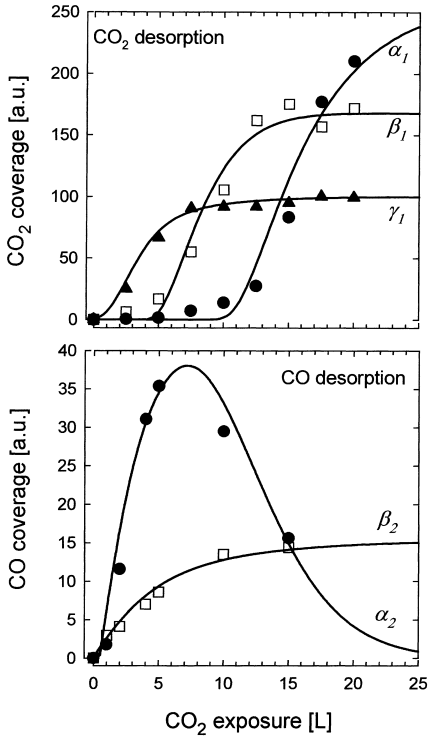

Fig. 4. Evolution of the integrated intensity of each of the desorption peaks as the exposure to CO_2 increases. Upper part, CO_2 desorption, α_1-peak (∼210 K); β_1-peak (∼500 K) and γ_1-peak (∼700 K). Lower part, CO desorption, α_2-peak (∼230 K) and β_2-peak (∼310 K). Symbols, experimental data; continuous curves, the fitting with the statistical model proposed. More details in text.

foil showed the characteristic rolling texture with the (1 0 0) plane parallel to the surface. Taking all this into account in order to develop the model, we additionally postulate: (i) the CO_2 molecule can adsorb on both site types but if it adsorbs on a *b*-site having neighboring empty *h*-sites it will move to these sites, where it decomposes; (ii) if when dissociation proceeds there is an empty first neighbor *b*-site, the formed CO molecule can jump and adsorb on it. Otherwise, the CO molecule remains on the *h*-site; (iii) the three CO_2 desorption peaks are assigned as follows: the α_1-peak, to desorption from multilayers, the β_1-peak, to desorption from *b*-sites and the γ_1-peak, to desorption from *h*-sites of rebuilt molecules after recombination of CO + O and (iv) of the two CO desorption peaks, the α_2 corresponds to *b*-sites, while the β_2 to *h*-sites. Accordingly, the following differential equations can be proposed, which represent the change upon exposure ε of the integrated intensity (coverage) of the γ_1 and β_1 desorption peaks of CO_2:

$$\frac{\mathrm{d}\theta_{\gamma}^{CO_2}}{\mathrm{d}\varepsilon} = k_1\left[\frac{1}{3}(1-\theta_{\gamma}^{CO_2})+\frac{2}{3}(1-\theta_{\beta}^{CO_2})(1-(\theta_{\gamma}^{CO_2})^2)\right] \quad (1)$$

$$\frac{\mathrm{d}\theta_{\beta}^{CO_2}}{\mathrm{d}\varepsilon} = k_2\left[\frac{2}{3}(1-\theta_{\beta}^{CO_2})(\theta_{\gamma}^{CO_2})^2\right] \quad (2)$$

In Eq. (1) the term $(1/3)(1-\theta_{\gamma}^{CO_2})$ is the probability for a CO_2 molecule to impinge on an unoccupied *h*-site and the term $(2/3)(1-\theta_{\beta}^{CO_2})(1-(\theta_{\gamma}^{CO_2})^2)$ is the probability for a CO_2 molecule to impinge on a *b*-site which has an empty first neighbor *h*-site. Consequently, Eq. (2) represents the probability for a CO_2 molecule to impinge on a *b*-site having the two neighboring *h*-sites occupied. Parameters k_1 and k_2 are proportionality constants ($k_1 = k_2$). According to the proposed postulates, the functions $\theta_{\alpha}^{CO_2}(\varepsilon)$, $\theta_{\alpha}^{CO}(\varepsilon)$ and $\theta_{\beta}^{CO}(\varepsilon)$ can be evaluated through the following set of equations:

$$\theta_{\alpha}^{CO_2}(\varepsilon) = k_3[\theta_{\beta}^{CO_2}(\varepsilon)]^4[\theta_{\gamma}^{CO_2}(\varepsilon)]^4 \quad (3)$$

$$\theta_{\alpha}^{CO}(\varepsilon) = k_4(\theta_{\gamma}^{CO_2}(\varepsilon)) - [1-(\theta_{\beta}^{CO_2}(\varepsilon))^4] \quad (4)$$

$$\theta_{\beta}^{CO}(\varepsilon) = k_5[\theta_{\gamma}^{CO_2}(\varepsilon)] \quad (5)$$

The right side of Eq. (3) gives the probability that all the *b* and *h*-sites are occupied, a necessary statement for the multilayer adsorption of CO_2, and consequently the evolving of the α_1-peak. Eq. (4) establishes that CO_2 molecules only dissociate on *h*-sites, and that the integrated intensity of the α_2-peak of CO desorption depends on the availability of empty neighboring *b*-sites onto which the CO molecules jump and remain adsorbed until desorption temperature is reached. Finally, Eq. (5) indicates that the occupation of *h*-sites with CO_2 molecules determines the integrated intensity of the β_2-CO peak. Parameters k_3 to k_5 are proportionality constants. The differential Eqs. (1) and (2) were numerically solved by means of the Runge-Kutta method (fourth order) in order to obtain $\theta_{\beta}^{CO_2}(\varepsilon)$ and $\theta_{\gamma}^{CO_2}(\varepsilon)$. With these functions and the aid of Eqs. (3)–(5), $\theta_{\alpha}^{CO_2}(\varepsilon)$, $\theta_{\alpha}^{CO}(\varepsilon)$ and $\theta_{\beta}^{CO}(\varepsilon)$ can be calculated.

The results of the fitting procedures are shown by the continuous lines in Fig. 4. Evidently, the model fits the experimental data fairly well in both cases, CO_2 and CO desorption. Especially interesting is the fact that the CO desorption is correctly described in spite of the presence of oxygen atoms on the surface, supporting in this way that the CO α_2-peak stems from molecules which jumped to empty bridge sites surrounding the hollow site where the CO_2 molecules had decomposed (Eq. (4)).

3.2. Desorption energies

In this section the most probable values for the desorption energies and their standard deviation are calculated. We have stated previously [12] that FTD spectra can be deconvoluted with Gaussian functions using the Marquard-Levenberg algorithm (commercial software) as Figs. 2 and 3 show. The width of the Gaussians was set to a fixed value because it depends only on the desorption energy distribution, e.g. it depends on the characteristics of the adsorbent surface, which remained constant throughout *all* the experiments (the same foil thoroughly annealed by ∼1500 K was used, checking a same starting surface structure by measuring the absolute photoelectric WF). Note that desorption peaks are broad, e.g. in Fig. 2 (CO_2 desorption) the FWHM involve ∼200 K (or more in peak γ_1). This fact prevents invoking adsorbate–adsorbate interactions in data interpretation due to the small energies involved in this case. In other words, the width is a consequence of the substrate polycrystallinity conferring a different environment to each adsorption site *of the same type*. Consequently, it can be proposed that *each type of site* shows a continuous normalized distribution function of desorption energies $f(\mathcal{E})$. Let N_s be the total number of sites of the same type and N_a the number of particles adsorbed at the time $t = 0$, (i.e. previous to FTD) therefore a global coverage can be defined as $\Theta = (N_a/N_s)$. It is also possible to define a local coverage $\theta_{\mathcal{E}_i} = n_{ai}/n_{si}$, where n_{ai} is the number of molecules adsorbed on n_{si} sites of the same type (which are a portion of the total number of sites N_s of the same type) defined by $n_{si} = f(\mathcal{E}_i)N_s$. The molecules adsorbed in these sites show desorption energies in the range $\mathcal{E}_i$ and $\mathcal{E}_i + d\mathcal{E}_i$. The probability that a molecule prior to desorption diffuses from a site with adsorption energy $\mathcal{E}$ to another with energy $\mathcal{E}'$ is extremely low due to the high heating rates used (∼100 K/s). Consequently, each desorption process from a state characterized by the adsorption energy $\mathcal{E}_i$ takes place independently of all other states and the *local* desorption rate will follow the Polanyi-Wigner equation [19]:

$$-\frac{d\theta_{\mathcal{E}}}{dt} = \nu^n \theta_{\mathcal{E}}^n \exp\left(-\frac{\mathcal{E}}{kT}\right) \tag{7}$$

or, in the case of the global desorption rate:

$$-\frac{d\Theta}{dt} = \nu^n \Theta^n \exp\left(-\frac{E_d}{kT}\right). \tag{8}$$

Taking into account that:

$$N_a = \int_0^\infty n_{ai}\, d\mathcal{E}_i = N_s \int_0^\infty \theta_{\mathcal{E}_i} f(\mathcal{E}_i)\, d\mathcal{E}_i \tag{9}$$

the relation between global and local coverage is:

$$\Theta = \int_0^\infty \theta_{\mathcal{E}} f(\mathcal{E})\, d\mathcal{E} \tag{10}$$

and Eq. (8) can be written as:

$$-\frac{d\Theta}{dt} = \int_0^\infty \nu^n \theta_{\mathcal{E}}^n f(\mathcal{E}) \exp\left(-\frac{\mathcal{E}}{kT}\right) d\mathcal{E} \tag{11}$$

If the FTD is performed with a linear heating rate β, the global desorption rate can be written:

$$-\frac{d\Theta}{dT} = \int_0^\infty \frac{1}{\beta} \nu^n \theta_{\mathcal{E}}^n f(\mathcal{E}) \exp\left(-\frac{\mathcal{E}}{kT}\right) d\mathcal{E} \tag{12}$$

in which n is the reaction order and ν the striking frequency of the molecule against the potential desorption barrier. Eq. (12) provides two different types of results: (i) when from a specific distribution function $f(\mathcal{E})$, the global desorption rate $-d\Theta/dT$ is calculated, or (ii) when from the global desorption rate the energy distribution function is determined. The former requires the integration of Eq. (12), and the latter the solution given by Seebauer [20], who proposed the following distribution function:

$$f(\mathcal{E}) = \frac{1}{\Theta_0} \left(\frac{T}{\mathcal{E}(T)}\right) \frac{d\Theta}{dT} \tag{13}$$

in which the initial coverage Θ_0, as well as $d\Theta/dT$, are obtained from the integrated intensity and the

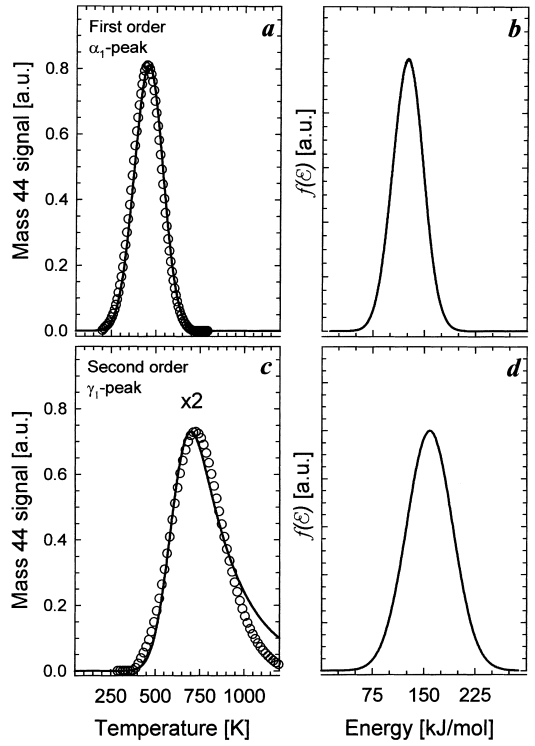

Fig. 5. Fitting of CO_2 desorption peaks after 15 L exposure, considering a Gaussian distribution of adsorption energies $f(\mathcal{E})$: (a) assuming first order kinetics for the CO_2 β_1-peak and (b) assuming second order kinetics for the CO_2 γ_1-peak. From the curves (a) and (c), the $f(\mathcal{E})$ distribution functions (b) and (d) are calculated, according to Eqs. (13) and (14). In turn, from these functions, the global desorption rates given by the circles in (a) and (b) were calculated. More details in text.

global desorption rate of the desorption peak. The energy $\mathcal{E}(T)$ can be obtained from the relation proposed by Redhead [19]:

$$\frac{\mathcal{E}}{kT^2} = \left(\frac{\nu}{\beta}\right)(\theta_{\mathcal{E}}^0)^{(n-1)} \exp\left(-\frac{\mathcal{E}}{kT}\right) \quad (14)$$

From the deconvoluted desorption spectra, $(-\mathrm{d}\Theta/\mathrm{d}T$ versus $T)$, the distribution function was obtained solving Eq. (14) for each T in Eq. (13), assuming a first order kinetic for the α and β-peaks of CO_2 or CO, but a second order for the CO_2 γ_1-peak. Fig. 5 shows the results in the case of CO_2. From the curves (a), first order and (c), second order, the $f(\mathcal{E})$ distribution functions (b) and (d) are calculated. In turn, with the $f(\mathcal{E})$ obtained, the FTD spectra were calculated, which are represented by the circles in (a) and (c). Note that the experimentally obtained high temperature tail in Fig. 5c is not correctly reproduced only assuming a Gaussian $f(\mathcal{E})$ for a second order reaction. This fact can be considered as an indication that the best fitting to the experimental data which required an exponential modified Gaussian, as shown in Fig. 2, is not due to the second order reaction but stems from the presence of other type of adsorption sites than those proposed in the model, as explained in the experimental part. These site types were not considered *directly* in the model because of their low surface density, but *indirectly* when postulating a continuous energy distribution function. In other words, the model clearly suggests that the high temperature tail in the CO_2 γ_1 desorption peak definitely cannot be interpreted as arising from a second order reaction (the recombination of CO + O).

From the fitting of all the desorption spectra as explained above and assuming $\nu/\beta \sim 10^{13}\,\mathrm{K}^{-1}$, the following desorption energies and standard deviations were obtained. For the CO_2: α_1-peak, $E_{d0} \sim 60.6$ kJ/mol ($\sigma \sim 16.3$ kJ/mol); β_1-peak, $E_{d0} \sim 126.9$ kJ/mol ($\sigma \sim 23.1$ kJ/mol); γ_1-peak, $E_{d0} \sim 158.7$ kJ/mol ($\sigma \sim 33.7$ kJ/mol). For the CO: α_2-peak, $E_{d0} \sim 73.1$ kJ/mol ($\sigma \sim 13.5$ kJ/mol); β_2-peak, $E_{d0} \sim 110.6$ kJ/mol ($\sigma \sim 20.2$ kJ/mol). The authors have no reference of CO_2 desorption energy data from Mo but the magnitude of some values in other metals are comparable to the present data [21].

4. Conclusions

Experimental data on FTD of CO_2 from polycrystalline Mo-foil can be quantitatively interpreted postulating that the surface has, principally, two types of adsorption sites to offer: bridge and hollow ones. This assumption is justified by the rolling texture of the foil established by XRD (crystal planes (1 0 0) parallel to the surface). Moreover, because of polycrystallinity, which gives different environments to sites even of the same type, wide distribution functions of adsorption energies for both types of sites can be proposed. The CO_2 molecule can adsorb on both site types but it is proposed that dissociates only on the hollow ones. Based on these postulates, a set of equations conform the model which allows the fol-

lowing global interpretation of the desorption process: (i) the α_1-CO_2 desorption peak at $T \sim 215\,K$ corresponds to those molecules adsorbed in multilayers (cf. Eq. (3)). (ii) From the chemisorbed CO_2 species, those on bridge sites constitute the β_1-peak desorbing at $T \sim 480\,K$ without suffering dissociation. (iii) The CO_2 molecules on hollow sites suffer dissociation in CO + O but those, which at the moment of dissociation were first neighbors of empty bridge sites, give rise to the CO α_2 desorption peak (cf. Eq. (4)). From the remaining CO molecules, a fraction desorbs in the β_2-peak while the rest rebuild CO_2 in a second order reaction, which desorbs in the γ_1-peak at $T \sim 700\,K$ (cf. Eq. (5)). (iv) The proposed model also interprets the maximum amount of CO molecules desorption occurring at CO_2 exposures of $\sim$5 L (peak α_2 in Fig. 4b) and the dramatic decrease at higher exposures. Also the dependence on CO_2 coverage of the β_2-peak of CO, desorbing at $T \sim 400\,K$, is correctly described by the model.

Acknowledgements

The authors acknowledge the financial support of the Argentine Research Council (CONICET) as well as the donation of equipment by the A. von Humboldt-, the Volkswagen Werk-Foundations (Germany) and the International Program for Physical Sciences (IPPS, Sweden). L.D. L-C is also grateful to COLCIENCIAS (Colombia) and the International Center for Theoretical Physics (Italy) for financial assistance.

References

[1] G. Hess, H. Froitzheim, Ch. Baumgartner, Surf. Sci. 331–333 (1995) 138.
[2] G. Illing, D. Heskett, E.W. Plummer, H.-J. Freund, J. Somers, Th. Linder, A.M. Bradshaw, U. Buskotte, M. Neumann, U. Starke, K. Heinz, P.L. De Andres, D. Saldin, J.B. Pendry, Surf. Sci. 206 (1988) 1.
[3] J. Krause, D. Borgmann, G. Wedler, Surf. Sci. 347 (1996) 1.
[4] M. Pirner, R. Bauer, D. Borgmann, G. Wedler, Surf. Sci. 189/190 (1987) 147.
[5] F. Solymosi, G. Klivényi, Surf. Sci. 315 (1994) 255.
[6] B. Bartos, H.-J. Freund, H. Kuhlenbeck, M. Neumann, H. Linder, K. Müller, Surf. Sci. 179 (1987) 59.
[7] P.H. Dawson, J. Vac. Sci. Technol. 16 (1) (1979) 1.
[8] H.-J. Freund, R.P. Messmer, Surf. Sci. 172 (1986) 1.
[9] J. Haggin, Chem. Eng. News 8 (1982) 13.
[10] H. Körner, H. Landes, G. Wedler, H.J. Kreuzer, Appl. Surf. Sci. 18 (1984) 361.
[11] J.-W. He, W. K. Kuhn, D. W. Goodmann, Surf. Sci. 262 (1992) 351, and references therein.
[12] L.D. López-Carreño, J.M. Heras, L. Viscido, Surf. Sci. 377–379 (1997) 615.
[13] L.D. López-Carreño, J.M. Heras, L. Viscido, in: Proceedings of the Eighth Latin American Congress on Surface Science and its Applications, Cancun, Mexico, 19–23 September 1994, AIP Conf. Proc. 378 (1994) 658.
[14] J. Hölzly, F.K. Schulte, Work function of metals, in: Solid State Physics, Springer Tracts Mod. Phys., Vol. 85, Springer, Berlin, 1979.
[15] D.E. Eastman, Phys. Rev. B 2 (1970) 1.
[16] W. Heiland, E. Taglauer, Surf. Sci. 68 (1977) 96.
[17] Powder Diffraction file 42-1120, JCPDS, International Center for Diffraction Data.
[18] H.P. Klug, L.E. Alexander, XRD Procedures, Wiley, New York, 1967.
[19] P.A. Redhead, Vacuum 12 (1962) 203.
[20] E.G. Seebauer, Surf. Sci. 316 (1994) 391.
[21] F. Solymosi, J. Mol. Catal. 65 (1991) 337.